Developing and analysing an electromechanical model of a bio-inspired flapping wing mini UAV

M. Park[1], A. Abolfathi[1*], J. D. Biggs[2], Y. Ventikos[1]
[1] University College London, Department of Mechanical Engineering
Roberts Engineering Building, Torrington Place, London, UK WC1E 7JE
[*] e-mail: **a.abolfathi@ucl.ac.uk**

[2] Politecnico di Milano, Department of Aerospace Science & Technology
Via La Masa 34, 20156 Milano, Italy

Abstract

The purpose of this paper is to describe and analyse an electromechanical model of a mini flapping wing mechanism for the purpose of system optimisation. The system comprises of a small DC motor connected to a voltage source, a gearbox and a slider crank that drives two wings. The DC gearmotor is modelled considering its both mechanical and electrical components. An equivalent viscous damper is considered to model the mechanical losses of the gearmotor. The crank mechanism is assumed massless and the inertia of the wings only considered in the model. The aerodynamic drag and lift are modelled using an equivalent viscous damping model as an energy sink. The parameters of the system are estimated using published experimental data and manufacturer datasheets for the corresponding DC gearmotor. The energy efficiency as the ratio of aerodynamic power to the input electrical power of the system and also the aerodynamic power are used as two measures to evaluate the system performance.

1 Introduction

Flying insects have evolved over millions of years and have become very successful species [1]. They are optimised flying machines which are outperforming any man-made air vehicles. In recent years, there have been several attempts to mimic the flapping wing mechanism of insects and to develop mini and micro Flapping Wing Unmanned Aerial vehicles (FWUAVs) [2,3]. It is suggested that the insect flight mechanism is a resonant oscillator that can exchange the kinetic and strain energy during a flapping cycle which allows most of the muscle energy being converted to the aerodynamic forces [4]. Similarly, any flapping wing mini aerial vehicle should be optimised in order to minimise the energy losses in the system and produce the highest possible lift. This can be achieved by adding an elastic energy storage element to the system and tuning the resonance frequency of the flapping system to match with the flapping frequency e.g. [5–10].

Madangopal et al. [6] designed a flapping wings mechanism using a four-bar mechanism. They attached a linear spring to the wings to mimic the energy storage mechanism of insect thorax. They investigated the energy consumption of the mechanism. Khan and Agrawal [8] provided a model of a four-bar flapping mechanism to which wings were attached using a rotational spring. Mechanical losses were assumed of viscous damping type and inertia of linkages and motor were included in their model. Khan and Agrawal [11] suggested an increase in the inertia of the motor to smooth the torque requirement of the flapping mechanism. Baek et al. [12] introduced an electromechanical model of flapping wing mechanism by assuming a single degree of freedom linear oscillator with viscous damping that modelled the flapping wing. They studied the nondimensional equations for different values of damping ratio and considered two cases of constant speed and constant current. They concluded that the battery and motor resistance have a considerable effect on the efficiency of the system. Lau et al. [13] manufactured two flapping wings mechanism of slider-crank type. One of them included an elastic storage mechanism and they showed that the mechanism with elastic element outperforms the conventional slider-crank mechanism in term of energy consumption.

In this paper, an electromechanical model of mini FWUAV powered by rotary DC motor is developed. This makes it possible to include effects of the electrical motor on the dynamics of the flying machine and to obtain the optimum parameters for the system. The main difference between the current study and the previous studies is the inclusion of the frictional losses in the hinges. This provides a platform to more accurately capture the dynamics of the system and enables accurate energy analysis.

2 Electro-Mechanical model

The rotary motion of a DC motor can be converted to the flapping motion of the wings through a crank and slider mechanism. A schematic view of such mechanism is shown in Figure 1 (a). The movement of the slider is confined to the vertical axis as shown in Figure 1 (b).

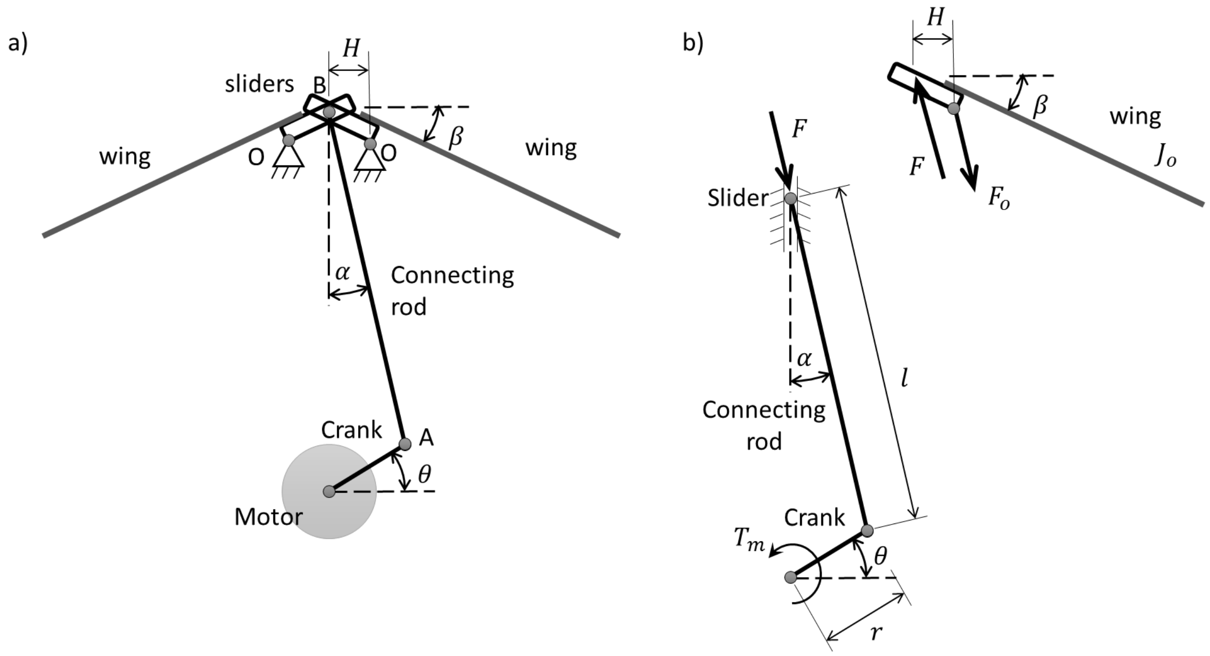

Figure 1: a) the schematic view of a flapping mechanism for a microdrone; b) Free body diagram of the wing and the crank and connecting rod, demonstrating the dimensions and the slider path of motion.

Assuming massless cranks and considering a viscous damping model to account for aerodynamic forces the equation of motion for the wings can be obtained as,

$$J_0\ddot{\beta} + c_a\dot{\beta} = FH(\sin\alpha\tan\beta + \cos\alpha) \tag{1}$$

where J_O is the combined moment of inertia of the wings about the hinge O, c_a is the equivalent aerodynamic damping coefficient. The counter clockwise direction and internal forces in tension are considered as positive directions. Geometrical parameters are defined in Figure 1. Angles α and β can be determined in terms of rotation of the crank θ. The equation of motion for the crank can be used to obtain the reaction force F in term of motor torque T_m,

$$T_m - T_f = Fr(\sin\theta\sin\alpha + \cos\theta\cos\alpha) \tag{2}$$

where T_f is the torque due to frictions in the hinges which accounts for mechanical losses in the flapping mechanism. The friction torque can be obtained by evaluating the reaction force,

$$T_f = F\mu r_e \tag{3}$$

where μ is the coefficient of friction and r_e is the effective radius. This formulation allows estimation of μr_e using experimental data which is described in the next section.

Coreless DC motors are commercially available at sizes that are suitable for mini air vehicles. The equivalent circuit of such a motor is shown in Figure 2 where R is the coil resistance, L is its inductance, e_{EMF} is the back electromotive force, T_1 is the coil torque, J_m is motor inertia, ω_1 is the motor speed, b_m is mechanical loss coefficient of the motor. Gear ratio is $1{:}n$, J_g is gear inertia, b_g is the gear loss coefficient, T_2 is gear torque and ω_2 is gear speed which is equal to $\dot{\theta}$.

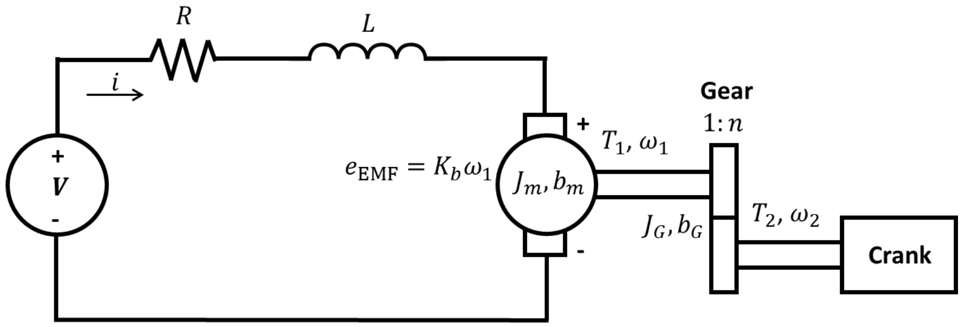

Figure 2: DC motor equivalent circuit.

The governing equations of the DC gearmotor can be obtained as,

$$V = L\frac{di}{dt} + Ri + e_{\mathrm{Emb}} \tag{4}$$

$$T_2 - T_m = (J_G + n^2 J_m)\frac{d\omega_2}{dt} + (b_G + n^2 b_m)\omega_2 \tag{5}$$

$$T_1 = K_b i \tag{6}$$

$$T_1\omega_1 = T_2\omega_2 \tag{7}$$

$$e_{\mathrm{EMF}} = K_b\omega_1 \tag{8}$$

As the mechanical losses of the gearmotor are estimated from the measurement provided by the manufacturer of the DC gearmotor, the mechanical losses of the gear and motor are substituted with an equivalent loss coefficient $b = b_G + n^2 b_m$. Equations (1) to (8) can be used to model the flapping drone in Matlab Simulink. The input to the model is the electrical voltage and the response of the system can be obtained. The model can be used to optimise the system as described in section 4.

3 Parameter estimation

Lau et al. [13] reported the experimental results on a flapping wing crank slider mechanism which are used to obtain the parameter for the simulations of this study. Their system incorporated a DC gearmotor (Precision Microdrive 206–102) for which the performance curves are produced by the manufacturer [14].

Using the manufacturer data, the parameters of the gearmotor are obtained which enabled to replicate the measured performance curves with an error of less than 5%. The estimated parameters for the gearmotor are given in Table 1.

Parameter	value
R	9.5 ohm
L	29×10^{-3} H
K_b	0.01 Nm/A
J	1.77×10^{-10} kgm^2
J_G	1×10^{-10} kgm^2
b	5×10^{-6} Ns
n	25

Table 1: Estimated parameters of DC gearmotor

The average power required to operate the flapping wing mechanism in different conditions is reported in reference [13]. The mechanical power of the system was measured running the flapping wings mechanism normally in the air, in a vacuum and when the wings were removed. This allowed a power analysis in absence of any elastic element by evaluating the total instantaneous power as the sum of inertia, aerodynamic and mechanical losses,

$$P_{\text{mech}} = P_{\text{aero}} + P_{\text{inertia}} + P_{\text{losses}} \tag{9}$$

where P_{mech} is the gearmotor output power, P_{aero} is the aerodynamic power, P_{inertia} is the inertia power required to accelerate and deaccelerate the masses of the system and P_{losses} are the mechanical losses in the system. The inertia power is of apparent power type and its average over a cycle is zero and does not contribute to the total power consumption of the system. However, it needs to be considered in the motor selection. It also increases the mechanical losses in the system due to an increase in reaction force hence the friction in joints. The average mechanical power can be obtained using the following equation,

$$\bar{P}_{\text{mech}} = \frac{1}{T}\int_T T_m \dot{\theta}\, dt \tag{10}$$

where T is the period. Similarly, the average aerodynamic power and the average mechanical losses power can be obtained,

$$\bar{P}_{\text{aero}} = \frac{1}{T}\int_T c_a \dot{\beta}^2 dt \tag{11}$$

$$\bar{P}_{\text{losses}} = \frac{1}{T}\int_T F\mu r_e \dot{\theta}\, dt. \tag{12}$$

An initial estimate for friction losses parameter μr_e can be obtained by assuming a constant rotational speed ($\dot{\theta} = 2\pi f$ where f is flapping frequency) and evaluating an average reaction force and comparing it with the measurement result of the mechanical power when the wings were removed in reference [13]. Similarly, the values for damping term c_a is obtained by evaluating the difference between the measured power of the system running in the air and running in the vacuum. The initial value can be obtained by assuming the increased mechanical losses is negligible and the difference can be approximated as the aerodynamic power given by equation (11). The estimations are updated through an iterative process taking into account the effect of increased losses to match the simulation results with the measurements. The dimensions of the flapping wing system and the estimated parameters are given in Table 2. The simulation results and measurements for the mechanical power and the total input electrical power are compared in Figure 3. The simulation can model the real system with a good accuracy.

Parameter	value
r	5 mm
l	20 mm
H	6 mm
J_o	7.205×10^{-8} kgm^2
c_a	1.8×10^{-5} Ns
μr_e	1.3×10^{-3} m

Table 2: Flapping wing mechanisms parameters values. r, l, H and J_o are adopted from reference [13] and c_a and μr_e are estimates.

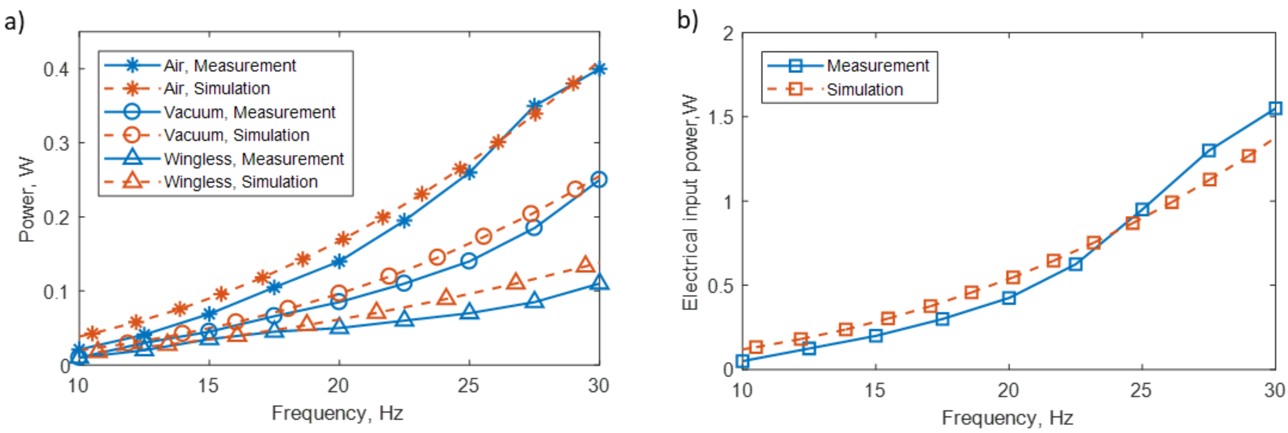

Figure 3: Mechanical power and input electrical power as a function of flapping frequency; solid lines: measurement result reproduced after [13], dashed lines: simulation results. a) Mechanical power of the flapping mechanism operating in the air, in a vacuum and when wings are removed. b) Input electrical power when the system operates in air.

4 Optimisation

Parameters of the system can be optimised using the model developed in this paper. The two important measures of performance for a flying machine are the energy efficiency and the aerodynamic power. The energy efficiency is defined as the ratio of aerodynamics power to the input electrical power here. The power dissipated through the viscous damper c_a can be considered as a measure of aerodynamic lift. The crank length is considered here first. The minimum size for the moving parts are dictated by manufacturability and crank length of 5 mm was used in the model of this study. It should be noted that the crank and the connecting rod are assumed massless and the effect of its increased mass and inertia is not considered here. The flapping angle is kept constant to compare just the effect of the length of cranthe k on the performance of the system. The efficiency and aerodynamic power are plotted in Figure 4 for three different input voltages as a function of the crank length.

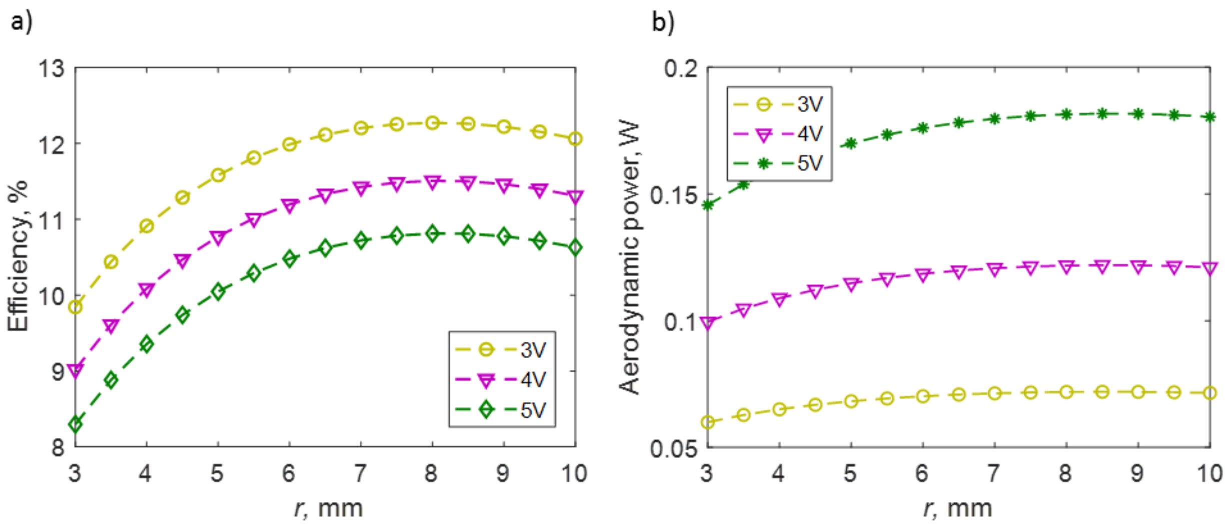

Figure 4: The efficiency and the aerodynamic power as a function of crank length for three different input voltages. a) Efficiency, b) aerodynamic power.

The efficiency and aerodynamic power increase with increasing the crank length initially and the maximum can be achieved for a length of 8 mm in this case. For lengths larger than 7 mm the aerodynamic power is almost constant. The highest efficiency can be achieved with an input voltage of 3 V. However, the aerodynamic power for this voltage is lower than the other two as expected. The higher efficiency for an input voltage of 3V is a result of the motor design which is tuned to operate at this voltage. The effect of changing the length of the connecting rod l on the system performance is shown in Figure 5. Increasing the length l cause a sharp increase in the efficiency for smaller lengths but the increase become smaller for larger lengths than 15 mm. Thus, a length of about 15 mm is a good compromise between the efficiency and the weight of the flying drone. The aerodynamic power is less sensitive to the changes in the connecting rod length after initan ial rapid increase for small lengths.

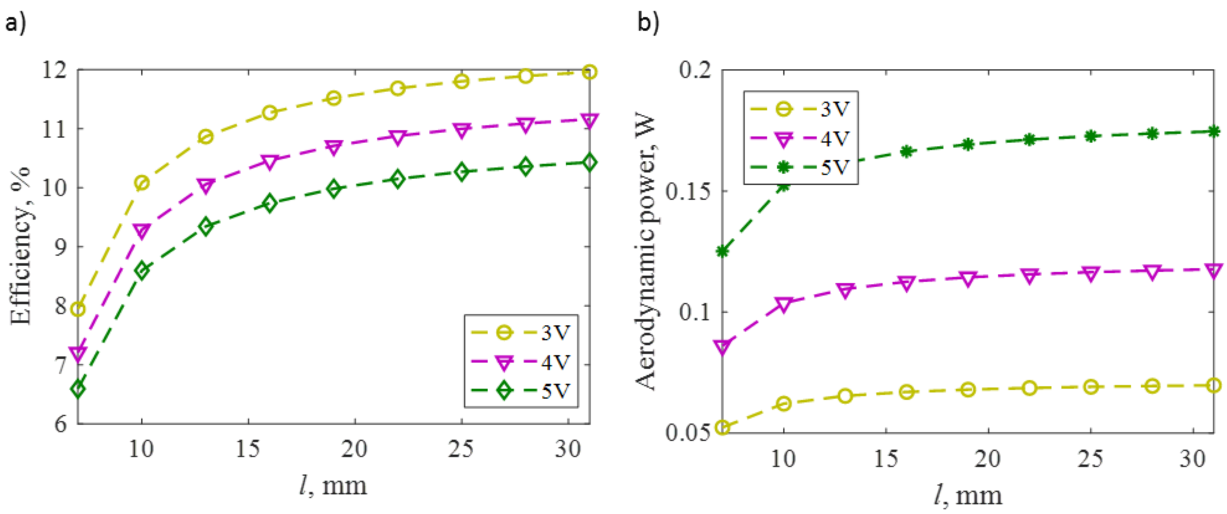

Figure 5: The efficiency and the aerodynamic power as a function of the length of the connecting rod l for three different voltages. a) Efficiency, b) aerodynamic power.

The size of the wings is very important for any flying machine as it is the interface between the mechanical power and the aerodynamic lift. It is important to know if the size that is chosen for a specific design is the optimum choice. The relation between the wing size and the lift is complex. Here, only a very simple viscous damper is used to model the aerodynamic lift. However, it is still possible to investigate how changes in the wing size can affect the performance of the system. For the sake of simplicity, it is assumed that the inertia of the wings J_o and the aerodynamic viscous damping coefficient c_a are linearly related. A ratio α is defined between the new values and nominal values for the wing inertia and the aerodynamic damping coefficient,

$$\alpha = \frac{c_a}{(c_a)_{\mathrm{nominal}}} = \frac{J_o}{(J_o)_{nominal}}. \tag{13}$$

The nominal values for c_a and J_o are given in Table 2. The efficiency and the aerodynamic power as a function of α are shown in Figure 6. By increasing α, the aerodynamic power increases as expected, however, the increased loads cause a decrease in the frequency of the flapping and changes in aerodynamic power become negligible for α greater than 0.7. Thus, a value of α about 0.9 which corresponds to maximum efficiency provides the optimum working condition.

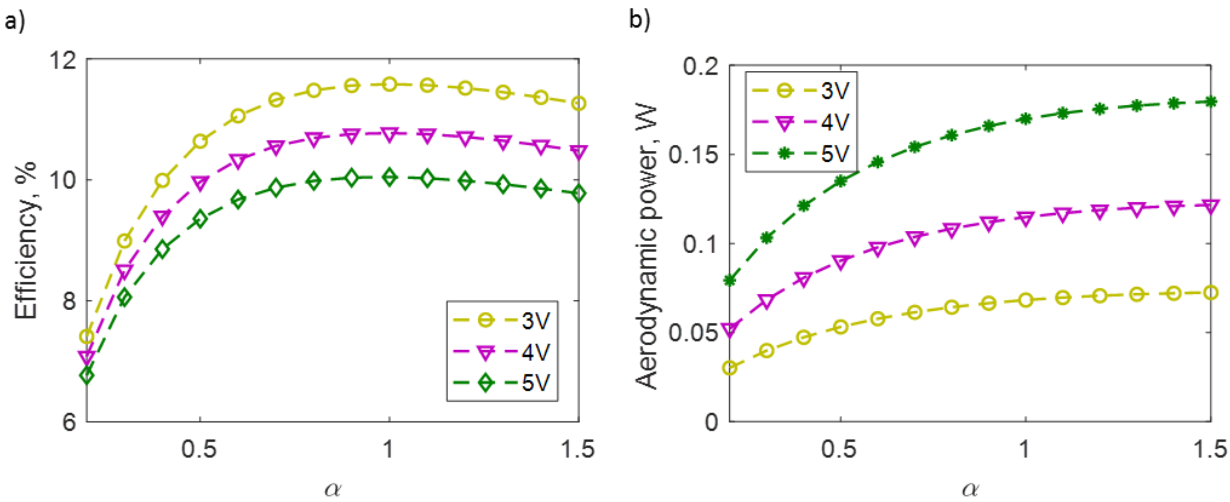

Figure 6: The efficiency and the aerodynamic power as a function of α for three different input voltages. a) Efficiency, b) aerodynamic power.

5 Conclusions

A mathematical model of a flapping wing mechanism is provided in this paper. The model includes two main parts, the electromechanical model of the DC gearmotor and the mechanical model of the flapping mechanism. A crank slider mechanism is used to convert the rotational motion to the flapping motion of the wings. The model includes the effect of friction which allows justifying the increase in losses due to inertia and aerodynamic forces. The parameters of the system are estimated using the published data and it is shown that the model can predict the experimental results with a good accuracy. The system efficiency and aerodynamic power are used as two measures of performance. The effects of the crank and connecting rod lengths on the performance of the system are investigated and optimum lengths are suggested. A linear relation between the inertia of the wing and the aerodynamic damping coefficient is assumed and the effect of changing the wing parameters on the performance is studied. A smaller size wing can slightly outperform the nominal size wing in term of the efficiency.

References

[1] C.P. Ellington, *The novel aerodynamics of insect flight: applications to micro-air vehicles*, Journal of Experimental Biology 202 (1999) pp. 3439-3448.

[2] D. Floreano, R.J. Wood, *Science, technology and the future of small autonomous drones*, Nature. 521 (2015) pp. 460–466. doi:10.1038/nature14542.

[3] G. Cai, J. Dias, L. Seneviratne, *A Survey of Small-Scale Unmanned Aerial Vehicles: Recent Advances and Future Development Trends*, Unmanned Systems, 02 (2014) pp. 175–199. doi:10.1142/S2301385014300017.

[4] C.H. Greenewalt, *The Wings of Insects and Birds as Mechanical Oscillators*, Proceedings of the American Philosophical Society, 104 (1960) 605–611. doi:10.2307/985536.

[5] G. Fischer, A.G. Cox, M.A. Gogola, M.K. Gordon, N.O. Lobontiu, D.J. Monopoli, E. Garcia, M. Goldfarb, *Elastodynamic locomotion in mesoscale robotic insects, in: Y. Bar-Cohen (Ed.), Smart Struct, in Proceedings Volume 3669, Smart Structures and Materials 1999: Electroactive Polymer Actuators and Devices*, Newport Beach, CA, United States, 1999, pp. 362–368. doi:10.1117/12.349694.

[6] R. Madangopal, Z.A. Khan, S.K. Agrawal, *Biologically Inspired Design Of Small Flapping Wing Air Vehicles Using Four-Bar Mechanisms And Quasi-steady Aerodynamics*, Journal of Mechanical Design, 127 (2005) 809. doi:10.1115/1.1899690.

[7] A. Cox, D. Monopoli, D. Cveticanin, M. Goldfarb, E. Garcia, *The Development of Elastodynamic Components for Piezoelectrically Actuated Flapping Micro-Air Vehicles*, Journal of Intelligent Material Systems and Structures 13 (2002) 611–615. doi:10.1106/104538902032463.

[8] Z.A. Khan, S.K. Agrawal, *Design of flapping mechanisms based on transverse bending phenomena in insects, in Proceedings 2006 IEEE International Conference on Robotics and Automation, Automn* 2006, ICRA 2006., IEEE, n.d.: pp. 2323–2328. doi:10.1109/ROBOT.2006.1642049.

[9] S. Avadhanula, R.J. Wood, D. Campolo, R.S. Fearing, *Dynamically tuned design of the MFI thorax, in Proceedings 2002 IEEE International Conference on Robotics and Automation (Cat. No.02CH37292),* 20002 11-15 May, Washington, DC, USA (2002) pp. 52–59. doi:10.1109/ROBOT.2002.1013338.

[10] E. Steltz, S. Avadhanula, R.S. *Fearing, High lift force with 275 Hz wing beat in MFI, in IEEE/RSJ International Conference on Intelligent Robots and Systems* 2007 29 Oct.-2 Nov., San Diego, CA, USA (2007), pp. 3987–3992. doi:10.1109/IROS.2007.4399068.

[11] Z.A. Khan, S.K. Agrawal., *Design and Optimization of a Biologically Inspired Flapping Mechanism for Flapping Wing Micro Air Vehicles, in: Proceedings 2007 IEEE International Conference on Robotics and Automation*, 2007 10-14 April, Roma, Italy, (2007), pp. 373–378. doi:10.1109/ROBOT.2007.363815.

[12] S.S. Baek, K.Y. Ma, R.S. Fearing, *Efficient resonant drive of flapping-wing robots, Efficient resonant drive of flapping-wing robots*, 2009 10-15 October, St. Louis, MO, USA, (2009), pp. 2854–2860. doi:10.1109/IROS.2009.5354725.

[13] G.-K. Lau, Y.-W. Chin, J.T.-W. Goh, R.J. Wood, *Dipteran-Insect-Inspired Thoracic Mechanism With Nonlinear Stiffness to Save Inertial Power of Flapping-Wing Flight*, IEEE Transactions on Robotics. 30 (2014), pp. 1187–1197. doi:10.1109/TRO.2014.2333112.

[14] DC Gearmotor | Precision Microdrives, https://www.precisionmicrodrives.com/product-catalogue/dc-gearmotor (accessed June 22, 2018).